International Journal of
INTELLIGENT SYSTEMS AND APPLICATIONS IN ENGINEERING
ISSN:2147-6799 www.ijisae.org Original Research Paper

Power Quality Improvement of Grid Integrated DFIG based Wind Power Conversion System with ANN-LSTM Controllers

Jyoti Prakash Jena[1], Sushil Kumar Bhoi[2*], Asini Kumar Baliarsingh[2]

Submitted:12/03/2024 **Revised**: 27/04/2024 **Accepted**: 04/05/2024

Abstract: Renewable energy sources connected to the grid for electric power generation are becoming more prevalent as they strive to meet the increasing demand for electricity without the use of fossil fuels. DFIGs are commonly utilized in wind turbines because they offer the benefit of being able to keep the frequency and amplitude of their produced voltages constant, regardless of the wind speed affecting the rotor of the turbine unit. Additionally, the DFIG offers a significant opportunity to enhance network dynamic performance through the utilization of power electronic converters equipped with adequate control systems. Various structure and control algorithms are available for regulating power converters. Traditional controllers are unable to operate at maximum efficiency when wind speed changes rapidly. Therefore, a new control technique utilizing ANN-LSTM controllers is introduced in this study to carry out various operations on grid-connected DFIG systems. The suggested control system has been evaluated across different voltage, frequency, reactive power load and wind speed variations. In order to obtain authentic responses, the Hardware-in-the-Loop (HIL) system is utilized alongside OPAL-RT modules to showcase comprehensive outcomes.

Keywords*: Renewable Energy Source; LSTM-ANN; Grid Connected Mode; DFIG; HIL; Power Quality.*

I. INTRODUCTION

Renewable energy sources are driving the adoption of electrical power generation to combat global warming. The global electricity generation from renewable energy sources is steadily rising to fulfill the increasing load demand without emitting any harmful gases [1-3]. Wind power is considered the most efficient renewable energy source for generating electricity due to its widespread availability across various locations. Wind power conversation units can be implemented in offshore and onshore locations for producing electrical energy. Wind energy conversion systems have a longer lifespan and entail minimal operating expenses. A turbine is primarily utilized to transform wind speed into mechanical energy, which is then harnessed as an input for an electrical generator to generate electricity. There are numerous generators that can be employed in a wind energy conversion system. In addition to numerous others, the doubly fed induction generator (DFIG) [4] with a back-to-back device is extensively utilized in high-power rating systems. DFIG units, with appropriate control mechanisms, have the capability to enable wind turbines to operate within a wide range of wind speeds. DFIG units are commonly employed in high power production systems. It is necessary to employ a back/back converting device technique in order to integrate a DFIG coupled wind power conversion unit into the utility grid, as a result of the variable wind speed. Therefore, it is essential to implement effective control mechanisms on these converters in order to enhance system stability and cost-effectiveness.

Several control strategies are utilized for converters, and most of these strategies involve the use of conventional proportional plus integral (PI) controllers. However, PI controllers may struggle to produce precise output when faced with sudden changes, as their fixed gains are set at a specific moment [5]. Therefore, it is essential to create artificial neural network (ANN) control methods in order to achieve optimal system performance in the face of unpredictable system variations. Nevertheless, traditional ANN controllers face challenges stemming from their limited memory capacity, which hinders their ability to store data for rapid processing in future iterations [6-7]. Furthermore, a wind turbine must be equipped with a maximum power point tracking (MPPT) system to optimize energy harvesting under various conditions. Hence, in this study, a novel integrated hybrid control method utilizing ANN-LSTM controllers has been devised for back-to-back circuits. This technique serves as a MPTT system for wind turbines and facilitates the transfer of active power to the grid. The active power produced needs to be fed into the utility grid, while also compensating for reactive power to operate local loads without drawing additional reactive power from the grid. This approach has the potential to enhance power quality as well. Additionally, accurately measuring the speed of a wind turbine is quite challenging. Hence, incorporating MPPTs sensorless control on the shaft of the DFIG can offer superior efficiency and cost savings. This paper utilizes ANN-LSTM controllers to implement a sensorless control method of MPPT on the rotor side

[1]*Department of Electrical Engineering, Biju Patnaik University of Technology Rourkela, Odisha*
[2]*Department of Electrical Engineering, Government College of Engineering Kalahandi, Bhawanipatna, Odisha*
*Email: [1]prakash11jena@gmail.com, *[2]sushilkumarbhoi@gmail.com, [2]asinikumar333@gmail.com*

converter (RSC) and a vector control with double loop on the grid side converter (GSC).

The paper is structured into the following parts. Section-II provides a description of the system, while Section-III presents the design of the ANN-LSTM controller. The recommended method is detailed in Section-IV. OPAL-RT technologies are employed in section-V to compress and present results with the assistance of HIL setup. The conclusion is provided in Section-VI, with the parameters of the various parameters used in the proposed unit being listed in the Appendix.

II. OUTLINE OF PROPOSED MODEL

Figure 1 illustrates the configuration of a grid-integrated DFIG unit with a back-to-back device. Two power electronic circuits are necessary, with one located on the rotor side and the other to be connected to the grid side through a transformer. Both converters must be linked together through a shared dc-link. A suitable MPPT approach is necessary to pinpoint the optimal power point. The Perturb and Observe (P&O) method is widely used, utilizing solely current and voltage to determine the optimal operating parameters for maximizing energy extraction. Therefore, the P&O algorithm is utilized on the RSC. Additionally, the speed sensorless technique has been implemented to calculate the DFIGs speed without the need for speed-measuring sensors. The management of power consumed by reactive loads is also implemented via the control system of the RSC. The GSC regulates the voltage across the dc-link, which is the voltage between two converters. Local side loads are managed on the load bus. A gear mechanism is integrated between the shaft of DFIG and wind turbine in order to uphold the necessary speed. The paper examines a two-mass model of a turbine based on references [2] in order to achieve more accurate responses. An 11kV system has been implemented, thus the DFIG is connected to the utility grid. Numerous scholars have recently put forward comparable systems, with a select few listed below.

The researchers in reference [8] successfully executed a synchronized control strategy and responsive current limitations for DFIG systems in the presence of asymmetrical grid situations. The stability analysis is discussed by the authors in [9] of a HVDC model-based grid-connected DFIG system. Authors in [10] implemented a DFIG system with sliding mode control by considering harmonically and unbalanced grid nature. The authors in [11] have developed a new MPPT and battery energy management system for grid connected DFIG system. The authors described in [12] have successfully deployed a Grid connected Battery-Wind-PV driven DFIG system to enhance power quality in diverse operational conditions. The authors in [13] have put forward a strategy for regulating the voltage of a DFIG system linked to a fragile grid through the use of an upgraded fractional order damping approach. The authors presented a fresh control strategy for the grid-integrated DFIG system in [14], which caters to multiple purposes and was also examined during faults and in isolated mode. The authors in [15] have implemented a cohesive power control method for DFIG system in standalone as well as grid mode. Nonetheless, authors have refrained from employing ANN-LSTM controllers to achieve enhanced response. Other authors did not take into account the power quality factors during random variations, nor did they apply a sensorless control method for MPPT of a wind turbine using the RSC of a DFIG unit.

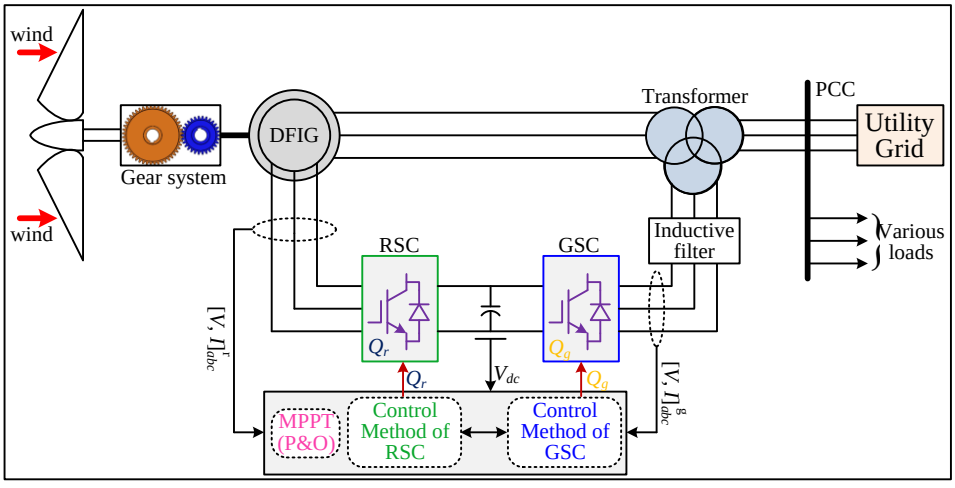

Fig 1: DFIG System integrated with utility grid.

This report is provided to meet the following array of objectives.

- Design ANN-LSTM controllers to utilize in proposed control methodology.
- The rotor side converter is utilized for sensorless control of MPPT in order to maximize power extraction from the wind turbine without the need for turbine speed sensing.
- The regulation of the DFIG speed is achieved by utilizing a rotor side converter for managing reactive power.

- The proposed control scheme on the grid side converter enables the compensation of reactive power for various loads operated at the point of common coupling (PCC).
- The proposed control method enhances power quality at the point of common coupling and ensures rapid response to unpredictable fluctuations in wind speed.

III. DESIGN OF ANN-LSTM CONTROLLERS

Efficient management of the power system necessitates the analysis, processing, validation, and storage of data. Therefore, the long short term memory (LSTM) algorithm based on artificial neural network (ANN) is utilized in this study from references [16-19]. LSTM is a model of recurrent ANN that is capable of learning long-term dependencies in data, making it well-suited for time series forecasting tasks. By incorporating LSTM into the ANN framework, the model is able to capture complex patterns and relationships in the data, leading to more accurate predictions. Additionally, LSTM has the ability to retain information over long periods of time, allowing it to make informed decisions based on historical data. Moreover, the utilization of LSTM in this study enhances the predictive capabilities of the model and provides valuable insights for decision-making processes. Additionally, a deep learning algorithm has been utilized to adjust the gains of the ANN model. Typically, the signals obtained from different areas within control units are often contaminated with grid-connected DFIG noise. To enhance the efficiency of the smart grid, it is essential to filter out any noise signals. The memory cells were added in the design of the controller based on ANN unit, as shown in Figure 2. The LSTM network's internal implementation is created through fundamental equations, with the layout depicted in Figure 3. The system's neurons' weights are updated in accordance with the requirements through the development of a machine learning (deep learning) algorithm. An unidentified sound signal (ns) is also taken into account as there could be a magnetic signal interference in the grid-connected DFIG system caused by high voltage and other elements. It is necessary to suppress these signals, therefore the opposite polarity has been considered for each element within the LSTM block.

$$a_t = (b_a + w_{ah} \times h_{t-1} + w_{ax} \times X_t \mp n_{sa}) \times \sigma \quad (1)$$

$$f_t = (b_f + w_{fh} \times h_{t-1} + w_{fx} \times X_t \mp n_{sf}) \times \sigma \quad (2)$$

$$O_t = (b_o + w_{oh} \times h_{t-1} + w_{ox} \times X_t \mp n_{so}) \times \sigma \quad (3)$$

$$\hat{C}_t = \tanh(b_c + w_{ch} \times h_{t-1} + w_{cx} \times X_t \mp n_{sc}) \quad (4)$$

$$s_t = f_t \otimes s_{t-1} + \hat{C}_t \times a_t \quad (5)$$

$$h_t = \tanh(s_t) \otimes O_t \quad (6)$$

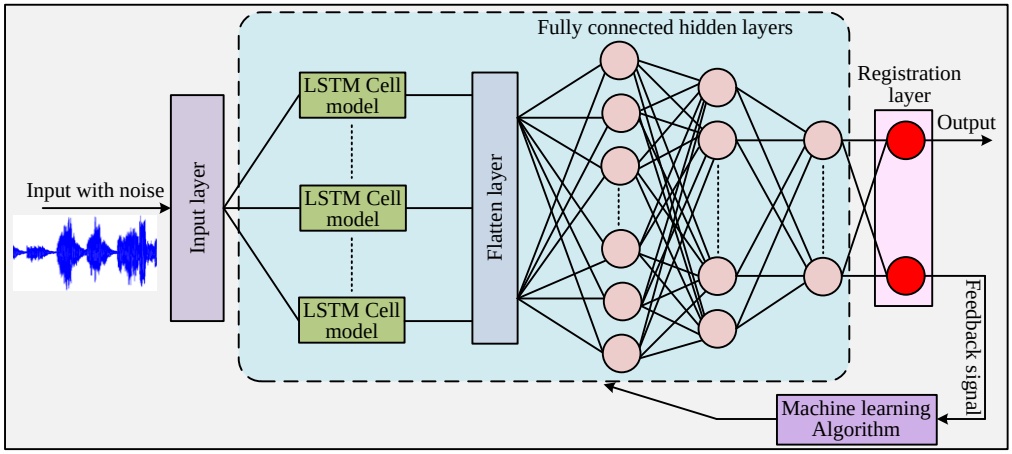

Fig 2: LSTM-ANN controlling model.

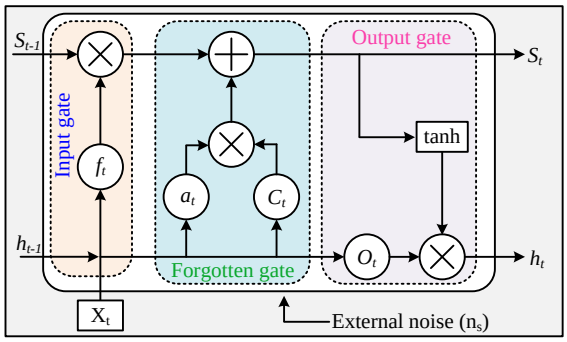

Fig 3: Model of a LSTM single cell.

Algorithm for LSTM Model.

Inputs: Data sheet of DFIG grid system, loads, and Converters →D_{pp}

Output: Predicted power Signals

Initialization: considered 'n' number of iterations ← {G_1, ……G_n}, 'l' number of load units ← {L_1, L_2, ……L_l}, etc.

Number of LSTM nodes: $N_{LSTM.}$

1: **Procedure** LSTM_Predictions.

2: Identification for Features from D_{pp}

3: **for** m←0 to n; l; etc

4: G_m[m] ← input1(); L_m[m] ← input2(); etc

5: **end for**

6: **for** m←0 to *n*; *l*; etc

7: Normalize G, L and other inputs in range {0, 1}

8: **end for**

9: **for** m←0 to *n*; *l*; etc

10: **if** {G_m[m]; L_m[m]; etc}.NotValid **then**

11: {inputs}←.Interpolate()

12: D_{pp}←duplicate_value

13: D_p←processed(D_{pp})

14: **end if**

15: **end for**

16: Proceed to all LSTM cells;

17: Output: Predicts_best_DPP_$LSTM_{layer}$_values

18: **end procedures.**

IV. PROPOSED CONTROL METHOD

This paper introduces new control methods for the RSC and GSC through the utilization of LSTM-ANN controllers. The P&O-based MPPT algorithm has been integrated into the control strategy of the RSC in order to function as an MPPT device for wind turbines by adjusting the DFIG's speed. The velocity of the DFIG is determined by analyzing the direct and quadratures (q&d) aspects of current and voltages. Therefore, this method has the capability to eliminate the need for an additional sensor to detect the speed of DFIG/wind turbine. The ANN-LSTM controllers have been designed for the purpose of estimating the necessary dq current components (I_{dqr}) on the rotor side of the DFIG. The reference components are further utilized to produce the necessary pulses for the rotor speed controller by following a hysteresis loop, as the rotor's speed can be adjusted by managing the rotor currents. The reference reactive power component required by DFIG is also taken into account, allowing the RSC to function as a reactive power source for the generator. Figure 4 illustrates the control scheme of RSC.

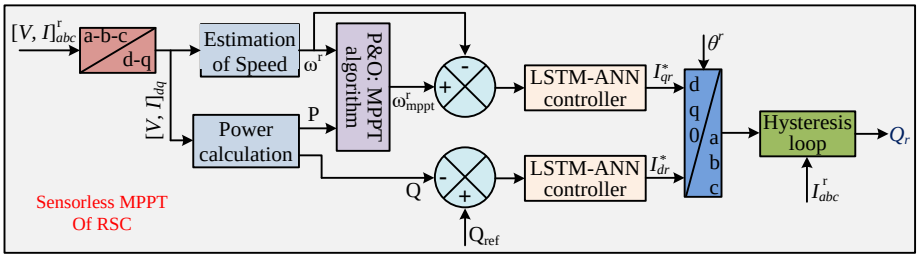

Fig 4: Proposed control methodology on RSC by using ANN-LSTM controllers.

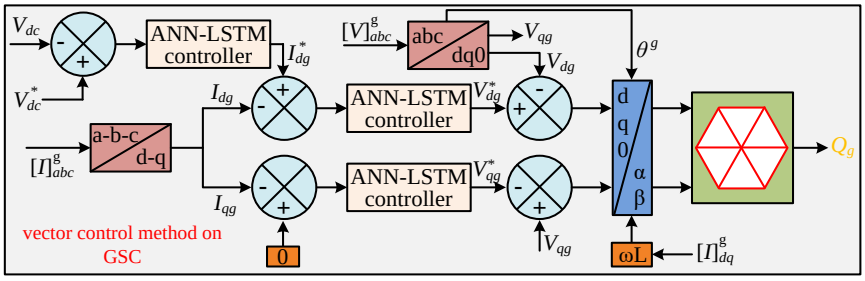

Fig 5: Proposed control methodology on GSC by using ANN-LSTM controllers.

Likewise, the GSC is integrated into the grid using a three-phase interface transformer. Utilizing ANN-LSTM controllers, a double loop vector control system has been put in place on GSC to uphold a steady dc-link voltage. The proposed control scheme integrates the grid currents to function as a device of reactive power compensator. The grid's reactive power component (Iq) is found to be zero, allowing the converter to fully offset the power demanded by the reactive loads. Thus, the grid is not required to compensate any reactive power demanded by load. Additionally, the suggested controller is capable of preserving power quality at the local load bus through the maintenance of a consistent voltage. Respective ANN-LSTM controllers are utilized to derive the reference d-q components of GSCs voltages. The Space Vector Pulse Width Modulation (SVPWM) method is employed for pulse generation, aiding GSC in achieving grid synchronization. The GSC's control scheme is depicted in Figure 5.

V. RESULTS AND DISCUSSIONS

The proposed configuration is implemented on the Simulink platform on the MATLAB software, employing a phasor type approach. Furthermore, the model has been partitioned into two sections to set up an HIL configuration with the OPAL-RT devices. To emulate real-time performance, real-time digital simulator (RTDS) units are employed to simulate the proposed model and present the outcomes. The

RTDS unit has ample capacity to solve complex power system equations in a manner similar to real-time operations, and it is widely recognized by scholars worldwide for testing power system models [1, 5]. The Real-Time Digital Simulator combines state-of-the-art computer hardware with comprehensive software. Both processing and communication modules are included in each unit.

Many researchers are using two RTDS modules based on microcontrollers/DSPs connected with suitable data cables to create the HIL configuration. OPAL-RT technologies have designed two RTDS modules which are connected through suitable channels to form a HIL for the designed configuration. Figure 6 displays the schematic depiction of the HIL setup incorporating the OPAL-RT module. The diagram in Figure 1 illustrates a division into two main components: the plant and the control unit. The plant model encompasses the grid, GSC, RSC, transformers, and loads, whereas the controller unit encompasses all control methods.

The signals from the plant's are converted into digital signals to be used as input for the control unit. The controller unit converts its output signals into analog signals, which are then utilized as input signals for the plant unit. Therefore, it established a complete circuit to evaluate the effectiveness of the suggested control methods in order to replicate the real-time model's response. The plant is processed by the RTDS unit, with the control scheme being carried out on the microcontroller. The full procedure of the HIL is carried out to evaluate the significance of the suggested control methods. The MATLAB software package is utilized to collect the responses of various signals in a computer for the purpose of examining the output waveforms.

During the testing of the model shown in Figure 1, an AC load bus is connected to the grid via a transformer, and multiple transmission lines are also taken into account to replicate real-time response. Version The 9MW DFIG system has been simulated using references [18-19], and the parameters of the system can be found in the Appendix. The model's design has been tested across a range of wind speeds. The performance of the proposed method is evaluated by taking into account the diverse changes and values of wind velocity. The wind turbine's speed is considered both above and below base speed. A speed of 12.0m/s is regarded as a threshold for the wind turbine. Therefore, if the speed exceeds the threshold speed, the pitch angle controller will activate to ensure the turbine operates correctly. The wind speed profile illustrated in Figure 7(a) clearly demonstrates ramp-like increases and decreases as the wind speed changes. This type of profile closely resembles real-time and includes a two-mass turbine model within the system. Consequently, there may be a delay in the pitch angle controller, leading to the attainment of slow turbine dynamics similar to those of a real-time model. The action of the pitch angle control system is illustrated in Figure 7(b).

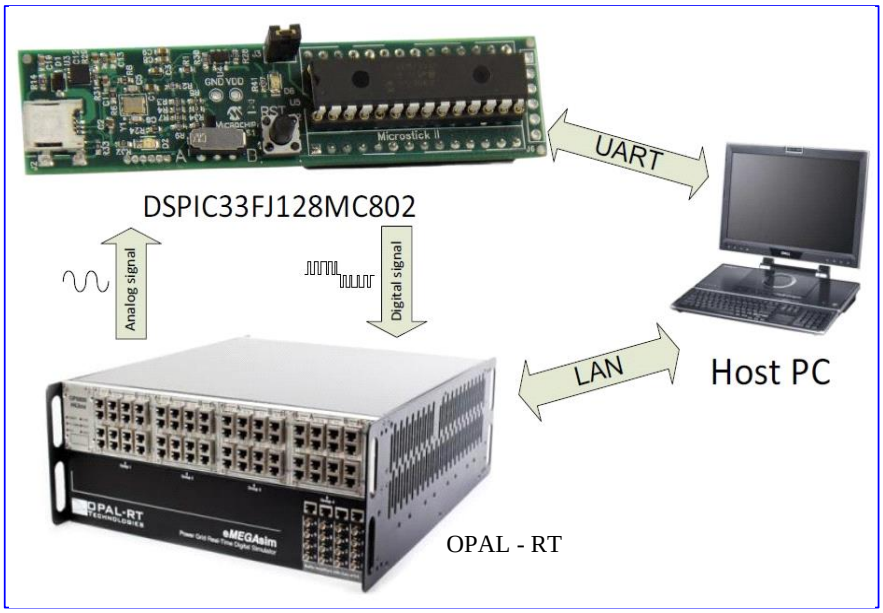

Fig 6: HIL configuration design with OPAL-RT Module.

The speed obtained by the DFIG unit (after the gear system) in per unit (p.u) is illustrated in Figure 7(c) as a result of the combined impact of pitch angle control and a two-mass wind turbine model. Figure 7(d) illustrates the voltage at the dc-link. When the wind speed exceeds the cutoff speed, there is a slight fluctuation in the dc-link voltage for a brief period. Nevertheless, the control strategies suggested for converters ensure that the dc-link voltage remains within the specified limit. The fluctuations in dc-link voltage do not exceed the specified limit. The phasor representation of the voltages generated by the DFIG can be observed in Figure 7(e). The voltage generated by DFIG remains relatively stable and within acceptable limits. A transformer is installed between the DFIG and the grid, along with transmission lines. An imbalanced load is being evaluated on the AC bus. Figure 7(f) illustrates the grid voltages that correspond to each other.

Grid voltages exhibit minimal fluctuations in response to variations in wind velocity, yet they remain predominantly stable. The real and reactive powers generated by DFIG can be found in Figure 7(g) for the real power and Figure 7(h) for the reactive power. The system is able to quickly and accurately respond thanks to the utilization of ANN-LSTM controllers when faced with sudden fluctuations in wind speed.

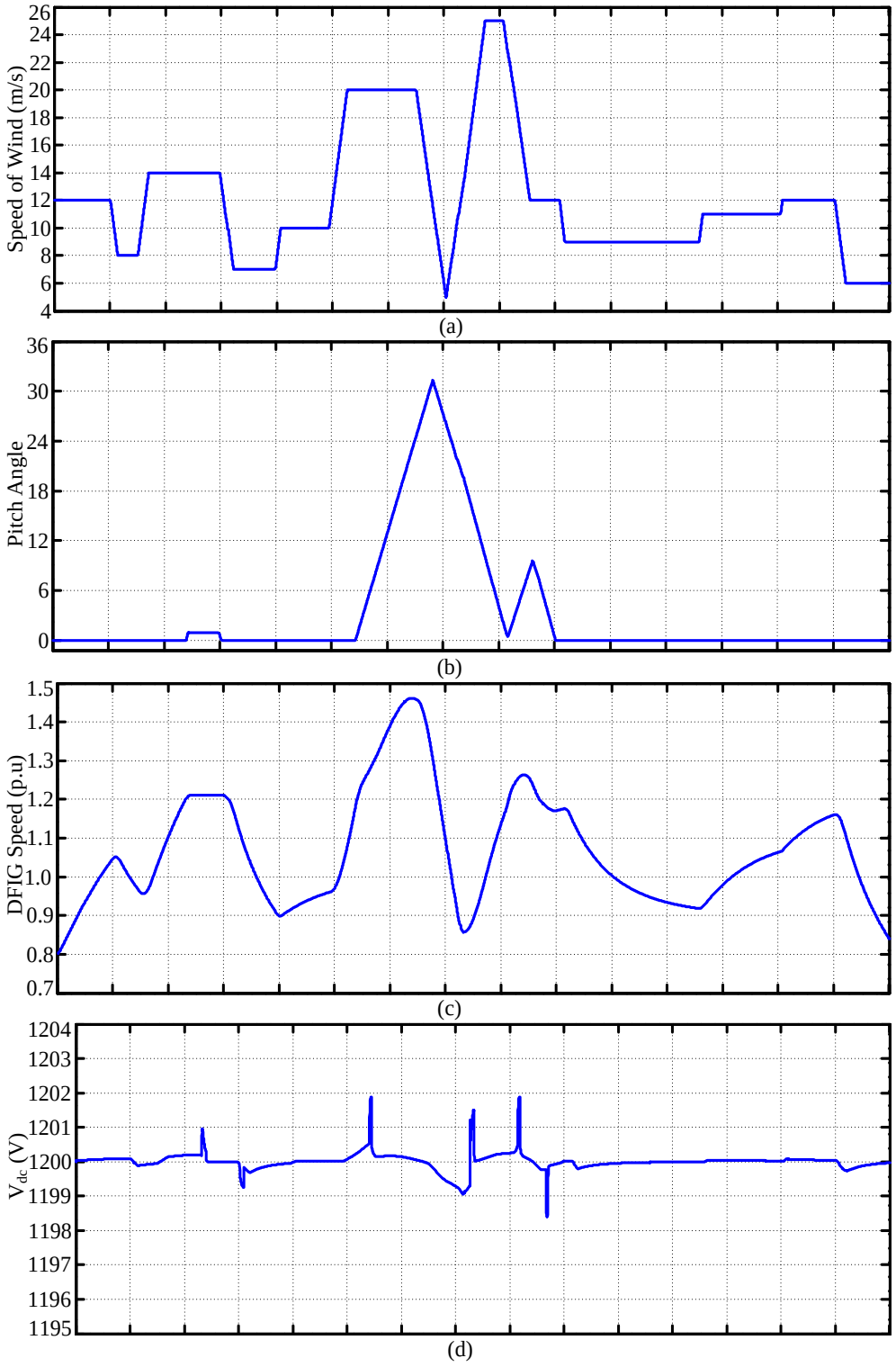

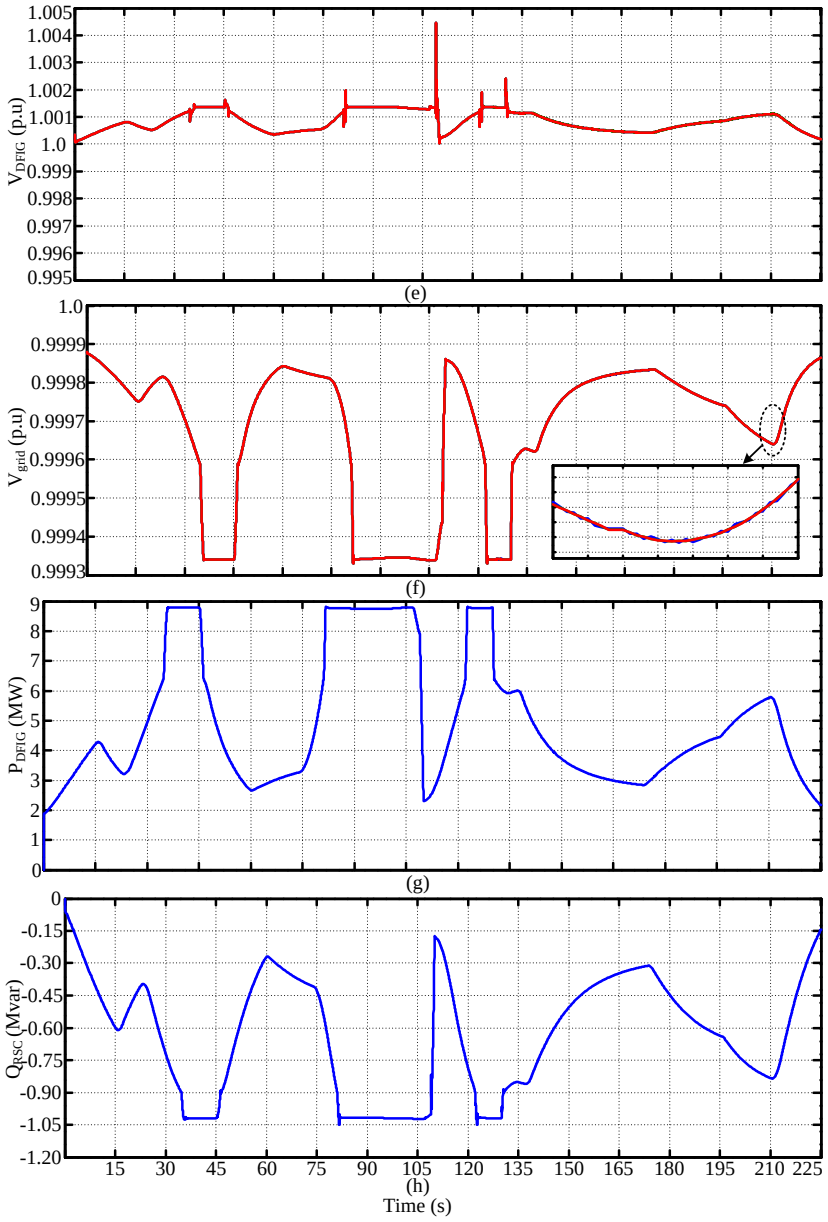

Fig 7: Under variations (a) Speed of wind, (b) pitch angle of blades, (c) DFIG shafts speed, (d) dc-link voltage, (e) DFIG voltages, (f) grid voltages, (g) P, and (h) Q.

VI. CONCLUSION

ANN-LSTM controllers are suggested for grid-connected DFIG systems in the study. The speed sensorless technique is utilized to develop the MPPT system for wind turbines using the RSC of the doubly fed induction machine based power generating unit. Therefore, the rotor side converter of a doubly fed induction generator can also function as the maximum power point tracker of a wind turbine. Reactive power compensation forms part of the control method of the GSC. An ANN approach utilizing machine learning is implemented to adjust the controller gains in order to enhance system responses when faced with fluctuations in wind speed. The responses are acquired through unpredictable fluctuations in wind speed due to ANN-LSTM controllers. OPAL-RT modules are employed to create a Hardware-in-the-Loop system to showcase the findings.

Appendix:

Table-I: Parameters of 9MW wind farm.

S.No	Parameters (Units)	Value
1	Power rating (MW)	9.0
2	Voltage (V)	575.0
3	Operating Frequency(Hz)	60.0
4	Resistance in stator winding (P.U)	0.0230
5	Resistance in rotor winding (P.U)	0.0160
6	Magnetizing inductance (P.U)	2.90
7	Leakage inductances of stator and rotor (P.U)	0.18; 0.16
8	Inertia constant	5.03
9	Number of pole pairs.	2.0
10	Maximum dc voltage (V)	1200.0

Table-II: Parameters of RSC & GSC.

S.No	Parameters (Units)	Value
1	Coupling inductors-GSC (P.U)	0.15
2	Capacitance (UF)	60000
3	Line resistance (P.U)	0.0015

Table-III: Data of wind turbine.

S.No	Parameter	Value
1	Mechanical power (MW).	9.5
2	Power at key point.	0.73
3	Wind speed at maximum power (m/s)	12.0
4	Pitch angle gain.	500
6	Maximum pitch angel.	45^0

Table-IV: Control parameters.

S.No	Parameter	Value
1	Reference voltage (P.U).	1.0
2	Droop X_s (P.U)	0.20
3	Rate of change of current (P.U/S)	200.0
4	Maximum number of neurons considered.	50.0

References

[1] Siva Ganesh Malla, et al., "Coordinated power management and control of renewable energy sources based smart grid" *International Journal of Emerging Electric Power Systems*, vol. 23, no. 2, 2022, pp. 261-276. https://doi.org/10.1515/ijeeps-2021-0113.

[2] S. G. Malla, P. K. Dadi and J. Dadi, "Wind and photovoltaic based hybrid stand-alone power generation system," 2017 International Conference on Energy, Communication, Data Analytics and Soft Computing (ICECDS), Chennai, India, 2017, pp. 3718-3725, doi: 10.1109/ICECDS.2017.8390158.

[3] Dash, D. P. Bagarty, P. K. Hota, U. R. Muduli, K. A. Hosani and R. K. Behera, "Performance Evaluation of Three-Phase Grid-Tied SPV-DSTATCOM With DC-Offset Compensation Under Dynamic Load Condition," in IEEE Access, vol. 9, pp. 161395-161406, 2021, doi: 10.1109/ACCESS.2021.3132549.

[4] M. Kumar, "A Review on Control Strategies for Wind Power Generation with DFIG for Smart Microgrid," 2021 International Conference on Control, Automation, Power and Signal Processing (CAPS), Jabalpur, India, 2021, pp. 1-6, doi: 10.1109/CAPS52117.2021.9730683.

[5] Malla, Priyanka, Malla, Siva Ganesh and Calay, Rajnish Kaur. "Voltage control of standalone photovoltaic – electrolyzer- fuel cell-battery energy system" *International Journal of Emerging Electric Power Systems*, 2022. https://doi.org/10.1515/ijeeps-2022-0047.

[6] Dash, et.al.,, "Harmonic Mitigation and DC Offset Rejection for Grid-tied DSTATCOM with CESOGI-WPF Control," 2022 3rd International Conference on Smart Grid and Renewable Energy (SGRE), Doha, Qatar, 2022, pp. 1-6, doi: 10.1109/SGRE53517.2022.9774064.

[7] J. -M. Won and F. Karray, "Necessity of parametric conditions for monotonic TSK fuzzy systems," 2012 IEEE International Conference on Systems, Man, and Cybernetics (SMC), Seoul, Korea (South), 2012, pp. 2026-2029, doi: 10.1109/ICSMC.2012.6378036.

[8] H. Xu, Y. Zhang, Z. Li, R. Zhao and J. Hu, "Reactive Current Constraints and Coordinated Control of DFIG's RSC and GSC During Asymmetric Grid Condition," in IEEE Access, vol. 8, pp. 184339-184349, 2020, doi: 10.1109/ACCESS.2020.3029227.

[9] K. Sun, et.al., "Impedance Modeling and Stability Analysis of Grid-Connected DFIG-Based Wind Farm With a VSC-HVDC," IEEE Journal of Emerging and Selected Topics in Power Electronics, vol. 8, no. 2, pp. 1375-1390, June 2020, doi: 10.1109/JESTPE.2019.2901747.

[10] Susperregui, M. I. Martínez, G. Tapia-Otaegui and A. Etxeberria, "Sliding-Mode Control Algorithm for DFIG Synchronization to Unbalanced and Harmonically Distorted Grids," in IEEE Transactions on Sustainable Energy, vol. 13, no. 3, pp. 1566-1579, July 2022, doi: 10.1109/TSTE.2022.3166217.

[11] Hamid, I. Hussain, S. J. Iqbal, B. Singh, S. Das and N. Kumar, "Optimal MPPT and BES Control for Grid-Tied DFIG-Based Wind Energy Conversion System," in IEEE Transactions on Industry Applications, vol. 58, no. 6, pp. 7966-7977, Nov.-Dec. 2022, doi: 10.1109/TIA.2022.3202757.

[12] S. Bhattacharyya, S. Puchalapalli and B. Singh, "Operation of Grid-Connected PV-Battery-Wind Driven DFIG Based System," in IEEE Transactions on Industry Applications, vol. 58, no. 5, pp. 6448-6458, Sept.-Oct. 2022, doi: 10.1109/TIA.2022.3181124.

[13] Z. Xie, X. Gao, S. Yang and X. Zhang, "Improved Fractional-order Damping Method for Voltage-controlled DFIG System Under Weak Grid," in Journal of Modern Power Systems and Clean Energy, vol. 10, no. 6, pp. 1531-1541, November 2022, doi: 10.35833/MPCE.2020.000843.

[14] M. V. Gururaj and N. P. Padhy, "A Cost-Effective Single Architecture to Operate DC Microgrid Interfaced

DFIG Wind System During Grid-Connected, Fault, and Isolated Conditions," in IEEE Transactions on Industrial Informatics, vol. 16, no. 2, pp. 922-934, Feb. 2020, doi: 10.1109/TII.2019.2926672.

[15] C. Wu, P. Cheng, Y. Ye and F. Blaabjerg, "A Unified Power Control Method for Standalone and Grid-Connected DFIG-DC System," in IEEE Transactions on Power Electronics, vol. 35, no. 12, pp. 12663-12667, Dec. 2020, doi: 10.1109/TPEL.2020.2996267.

[16] Y. Zahraoui, T. Korõtko, S. Mekhilef and A. Rosin, "ANN-LSTM Based Tool For Photovoltaic Power Forecasting.," 2024 4th International Conference on Smart Grid and Renewable Energy (SGRE), Doha, Qatar, 2024, pp. 1-6, doi: 10.1109/SGRE59715.2024.10428969.

[17] L. Jiang, X. Wang, L. Wang, M. Shao and L. Zhuang, "A hybrid ANN-LSTM based model for indoor temperature prediction," 2021 IEEE 16th Conference on Industrial Electronics and Applications (ICIEA), Chengdu, China, 2021, pp. 1724-1728, doi: 10.1109/ICIEA51954.2021.9516151.

[18] J. Yang, D. De Montigny and P. Treleaven, "ANN, LSTM, and SVR for Gold Price Forecasting," 2022 IEEE Symposium on Computational Intelligence for Financial Engineering and Economics (CIFEr), Helsinki, Finland, 2022, pp. 1-7, doi: 10.1109/CIFEr52523.2022.9776141.

[19] R. Q. Mohammed, M. M. Abdulrazzaq, A. J. Mohammed, K. Mardikyan and M. Çevık, "Enhancing Smart Grid Efficiency: A Modified ANN-LSTM Approach for Energy Storage and Distribution Optimization," 2023 7th International Symposium on Multidisciplinary Studies and Innovative Technologies (ISMSIT), Ankara, Turkiye, 2023, pp. 1-5, doi: 10.1109/ISMSIT58785.2023.10304846.